Supporting Information

D'Alise et al. 10.1073/pnas.1105364108

SI Materials and Methods

Cell Sorting and Flow Cytometry. Ex vivo Tregs were sorted as B220$^-$, CD8$^-$, CD11b$^-$, CD4$^+$, and CD25high (Moflo) from NOD and B6g7 mice. From the same animals, naive T cells for in vitro conversion were sorted as B220$^-$, CD8$^-$, CD11b$^-$, CD25$^-$, CD4$^+$, and CD62Lhigh. For surface staining, fluorophore-labeled mAbs specific for CD4 (RM4-5), CD8 (5H10), CD19 (6D5), TCR-β (H57-597), CD25 (PC61), CD62L (MEL-14), CD45.1 (A20), CD45.2 (104), and CD73 (TY/11.8) were obtained from Biolegend. GARP mAb (YGIC86) was obtained from eBioscience. Samples were acquired with LSR II (BD Bioscience) and data were analyzed with FlowJo (Tree Star).

In Vitro Conversion Assay. Naive CD4$^+$GFP$^-$ or CD4$^+$CD25$^-$ CD62L$^+$ T cells were activated with anti-CD3/CD28–coated beads (Invitrogen) at a concentration of one bead per cell in the presence of 20 units/mL of recombinant human IL-2 (Proleukin; Chiron) with or without 25 ng/mL of recombinant TGF-β (PeproTech). After 4 d of culture, Foxp3$^+$ cells were detected by APC-conjugated anti-Foxp3 intracellular mAb (FJK-16; eBiosciences) according with the manufacturer's protocol. Cells were analyzed by flow cytometry on LSRII (BD Biosciences).

In Vitro Suppression Assay. CD4$^+$CD25$^-$ or CD4$^+$GFP$^-$ target cells were labeled with 10 μmol/L CFSE (Molecular Probes) in RPMI 1640 at the concentration of 10^6/mL at 37° for 20 min, washed, resuspended in complete culture medium (RPMI 1640, 10% FCS, 2 mmol/L L-glutamine, penicillin/streptomycin), and cultured at 2.5×10^4–10^5 cells/well in a round-bottom, 96-well plate (Corning). Stimulation was effected by addition 1.5 μg/mL anti-CD3 antibody in presence of APC cells at ratio 1:1. Proliferation was measured by incorporation of ^{3}H-thymidine (1 μCi in the last 18 h of culture) or by flow-cytometric analysis of CFSE dilution. Recombinant GARP (amino acids 20–627; Alexis Biochemicals) fused to the Fc portion of human IgG1 was added to the cultures of Treg–Teffector cells in concentrations from 0.1 to 5 μg/mL.

Gene-Expression Analysis. For microarray analysis, RNA was labeled and hybridized to GeneChip Mouse Genome M1.0 ST chips arrays. The image reads were processed through Affymetrix software to obtain raw data and normalized using the RMA algorithm implemented in the GenePattern software package (1). The cell populations analyzed were generated in duplicate or triplicate. Data were analyzed with the "Multiplot" module from GenePattern.

For the cluster analysis in Fig. 2 *B* and *C*, a matrix of correlation coefficients (258 × 258) was calculated for all genes of the Treg signature, on the basis of their expression values in the 178 total conditions. We performed *k*-means clustering on the Treg signature of 305 genes using correlation as the distance measure. Repeated probes belonging to the same gene were removed, resulting in 258 Treg signature genes. We performed 100 runs each for $k = 5{:}30$ clusters in Matlab. For each of the clusters generated we computed the median expression of cluster member genes in the B6g7/NOD TGF-Treg samples and in control samples. We focused on the top clusters that had the highest median expression difference only between B6g7/NOD TGF-Tregs and not in control samples. Among these clusters, a representative clustering result for $k = 10$ is shown in Fig. 2*C*.

For RNA quantitative analysis, in vitro converted cells from NOD and B6g7 mice were sorted in 500 μL of TRIzol. RNA was reverse transcribed with oligo(dT) primers and SuperScript polymerase (Invitrogen). Real-time quantitative PCR was performed using gene-specific fluorogenic assays (TaqMan; Applied Biosystems). Transcripts levels were normalized to the *Hprt* gene.

1. Reich M, et al. (2006) GenePattern 2.0. *Nat Genet* 38:500–501.

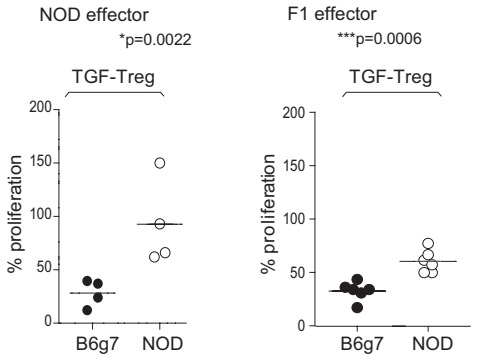

Fig. S1. The defect of NOD TGF-Tregs is irrespective of the source of T effector cells. Proliferation of T effector cells (measured by thymidine incorporation) isolated from NOD (*Left*) or F_1 mice (*Right*) was tested at ratio 1:1 with TGF-Tregs derived from NOD and B6g7 mice.

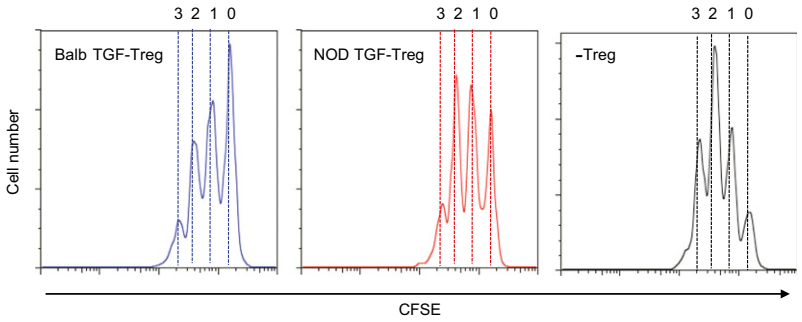

Fig. S2. The defect of TGF-Tregs is peculiar to NOD mice. Proliferation of T effector cells at ratio 1:1 Treg:Teff in presence of TGF-Tregs derived from NOD or BALB/c mice or in absence of Tregs (−Treg) is shown, tested by CFSE dilution.

Table S1. List of T-cell datasets related to cluster analysis of Fig. 2*B* datasets of Foxp3^{-}, Foxp3^{+}, and αβ T cells at different stages of differentiation from the Immgen consortium (1) used to perform a computational cluster analysis of Treg signatures genes

Dataset sample name	Dataset full name
T.4FP3+25+.Sp	Spleen Treg
T.4FP3+25+.LN	Lymphnode Treg
T.4FP3+25+.K_d	Kidney Tregs
T.4FP3+25+.Lung	Lung Tregs
T.4FP3+25+.Liver	Liver Treg
T.4FP3+25+.Skin	Skin Treg
T.4FP3+25+.ScAd	s.c. Treg
T.4FP3+25+.AbAd	Abdominal fat Treg
T.4FP3-.Sp	Spleen Tconv
T.4FP3-.LN	Lymph node Tconv
T.4FP3-.K_d	Kidney Tconv
T.4FP3-.Lung	Lung Tconv
T.4FP3-.Liver	Liver Tconv
T.4FP3-.Skin	Skin Tconv
T.4FP3-.ScAD	s.c. Tconv
T.4FP3-.AbAd	Abdominal fat Tconv
NOD TGF	TGF Treg NOD mice
B6 TGF	TGF Treg B6g7 mice
preT.ETP.Th	Early T lineage precursor
preT.DN1.Th	Double-negative 1
preT.DN2.Th	Double-negative 2
preT.DN3.Th	Double-negative 3
T.DN4.Th	Double-negative 4
T.ISP.Th	Immature single positive
T.DP.Th	Double-positive T cell
T.DPbl.Th	Double-positive blasts
T.DPsm.Th	Double-positive, small resting
T.DP69+.Th	Double-positive, early positive selection
T.4+8int.Th	Positive selection, intermediate
T.4int8+.Th	Positive selection, intermediate
T.4SP69+.Th	CD4 single-positive, intermediate
T.8SP69+.Th	CD8 single-positive, intermediate
T.8SP24int.Th	CD8 single-positive, semimature
T.8SP24-.Th	CD8 single-Positive, Mature
T.4SP24int.Th	CD4 single-positive, semimature
T.4SP24-.Th	CD4 single-positive, mature
T.4Nve.Sp	Spleen naive CD4
T.4Nve.LN	s.c. LN naive CD4
T.4Nve.MLN	Mesenteric LN naive CD4
T.4Nve.PP	Peyers patches naive CD4
T.4Mem.Sp	Spleen memory-phenotype CD4
T.4Mem.LN	s.c. LN memory-phenotype CD4
T.8Nve.Sp	Spleen naive CD8
T.8Nve.LN	s.c. LN naive CD8
T.8Nve.MLN	Mesenteric LN naive CD8
T.8Nve.PP	Peyers patches naive CD8
T.8Mem.Sp	Spleen memory-phenotype CD8
T.8Mem.LN	s.c. LN memory-phenotype CD8
T.4.Pa.BDC	Pancreas-infiltrating CD4, BDC islet-reactive TCR
T.4.PLN.BDC	Pancreatic LN CD4, BDC islet-reactive TCR Tg
T.4.LN.BDC	s.c. LN CD4, BDC islet-reactive TCR Tg
T.4.TI.B16	Tumor-infiltrating CD4, B16 melanoma
T.4.Sp.B16	CD4^{+}, spleen from B16 tumor-bearing
T.8.TI.B16	Tumor-infiltrating CD8, B16 sc
T.8.Sp.B16	CD8+, spleen from B16 tumor-bearing

1. Heng TS, Painter MW; Immunological Genome Project Consortium (2008) The Immunological Genome Project: Networks of gene expression in immune cells. *Nat Immunol* 9:1091–1094.

Table S2. List of Foxp3$^+$ T-cell populations related to analysis in Fig. 3*A*

Name	Full name
T.4FP3+25+.Sp	Spleen Treg
T.4FP3+25+.LN	Lymph node Treg
T.4FP3+25+.K_d	Kidney Tregs
T.4FP3+25+.Lung	Lung Tregs
T.4FP3+25+.Liver	Liver Treg
T.4FP3+25+.Skin	Skin Treg
T.4FP3+25+.Mu	Muscle Treg
T.4FP3+25+.ScAd	s.c. Treg
T.4FP3+25+.AbAd	Abdominal fat Treg
T.4+25+.blood	Blood Treg
T.4+25+.Sp	Spleen CD4$^+$CD25$^+$
NOD TGF	TGF-Treg NOD mice
B6 TGF	TGF-Treg B6g7 mice
T.4+25+.NOD Sp	NOD ex vivo Treg
T.4+25+.B6 Sp	B6g7 ex vivo Treg

Expression levels of *Lrrc32* were analyzed in several Foxp3$^+$ Tregs isolated from different locations (spleen, LN, blood, muscle, fat, skin, liver, kidney, and lung). The datasets included Foxp3$^+$ TGF-Tregs.